JOURNAL OF SOLID STATE CHEMISTRY **23,** 43–57 (1978)

Thermodynamic Properties of Fe–Lanthanoid–O Compounds at High Temperatures

TAKASHI KATSURA, TOSHIMORI SEKINE, KENZO KITAYAMA, AND TADASHI SUGIHARA

Department of Chemistry, Tokyo Institute of Technology, Ookayama, Meguro-ku, Tokyo 152, Japan

AND NOBORU KIMIZUKA

National Institute for Researches in Inorganic Materials, Sakura-mura, Niihari-gun, Ibaraki 300-31, Japan

Received March 17, 1977; in revised form June 2, 1977

After establishing the phase equilibria in the systems Fe–Fe_2O_3–Ho_2O_3 and Fe–Fe_2O_3–Tm_2O_3 at 1150, 1200, and 1250°C, the standard Gibbs free energies of formation of $HoFe_2O_4$, $Ho_3Fe_5O_{12}$, $HoFeO_3$, $TmFe_2O_4$, $Tm_3Fe_5O_{12}$, $TmFeO_3$ have been determined on the basis of reactions among metallic iron, oxygen, and the respective lanthanoid sesquioxide. A new compound $Tm_2Fe_3O_7$ was found at 1380°C. The standard Gibbs free energies of formation of $Gd_3Fe_5O_{12}$, $Tb_3Fe_5O_{12}$, and $Dy_3Fe_5O_{12}$ were also determined. On the basis of these new data together with our previous studies on phase equilibria in the Fe–Fe_2O_3–lanthanoid sesquioxide systems, we have been able to establish a phase diagram at high temperatures from 900 to 1400°C. The thermochemical relative stability in each type of compound, that is to say, $LnFeO_3$ (Ln = La, Nd, Sm, Eu, Gd, Tb, Dy, Ho, Er, Tm, Yb, Lu, and Y), $Ln_3Fe_5O_{12}$ (Ln = Sm, Eu, Gd, Tb, Dy, Ho, Er, Tm, Yb, Lu, and Y), $LnFe_2O_4$ (Ln = Ho, Er, Tm, Yb, Lu, and Y), and $Ln_2Fe_3O_7$ (Ln = Yb and Lu) was investigated by using the following standard Gibbs free energy changes of oxide–oxide reactions, $\frac{1}{2}Fe_2O_3 + \frac{1}{2}Ln_2O_3 = LnFeO_3$, $3LnFeO_3 + Fe_2O_3 = Ln_3Fe_5O_{12}$, $FeO + LnFeO_3 = LnFe_2O_4$, and $LnFe_2O_4 + LnFeO_3 = Ln_2Fe_3O_7$. The results thus obtained were compared with those of the structural relative stability.

Introduction

Recently, phase equilibria in the Fe–Fe_2O_3–Ln_2O_3 [Ln = La(1), Nd(2), Sm(2 and 3), Eu(2 and 4), Er(3), Yb(5), Lu(6), and Y(7)] systems have been established at 1200°C, and Kimizuka and Katsura (*5*) have proposed that these systems could be classified into four groups with respect to the assemblage of the ternary compounds. According to their proposal, the Fe–Fe_2O_3–(La and Nd)$_2O_3$ systems belong to the A type in which only one ternary compound $LnFeO_3$ exists stably, the Fe–Fe_2O_3–(Sm, Eu, Gd, Tb, and Dy)$_2O_3$ systems belong to the B type with two compounds $LnFeO_3$ and $Ln_3Fe_5O_{12}$, the Fe–Fe_2O_3–(Ho, Er, Tm, and Y)$_2O_3$ systems to the C type with three compounds $LnFeO_3$, $Ln_3Fe_5O_{12}$, and $LnFe_2O_4$, while the Fe–Fe_2O_3–(Yb and Lu)$_2O_3$ systems belong to the D type with four compounds $LnFeO_3$, $Ln_3Fe_5O_{12}$, $LnFe_2O_4$, and $Ln_2Fe_3O_7$. It is interesting that this classification depends wholly on the size of trivalent lanthanoid ions. Here, we show the four typical phase diagrams in Fig. 1.

The crystal structure analyses of $YbFe_2O_4$ and $Yb_2Fe_3O_7$ were performed by Kato *et al.* (*8*, *9*), and Kimizuka *et al.* (*10*) assert that there are homologous compounds $(LnFeO_3)_nFeO$ (n = 1, 2, 3, and 4) at high temperatures.

Katsura *et al.* (*2*) have studied some

0022-4596/78/2312-0043 $02.00/0

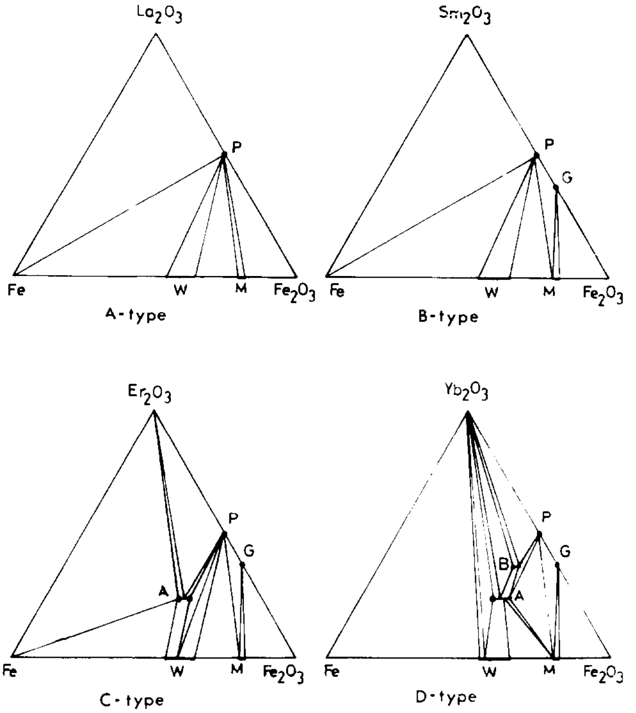

FIG. 1. The four typical phase diagrams of $Fe-Fe_2O_3-Ln_2O_3$ systems at 1200°C. P, perovskite ($LnFeO_3$); G, garnet ($Ln_3Fe_5O_{12}$); M, magnetite (Fe_3O_4); W, wüstite (FeO); A, $LnFe_2O_4$; and B, $Ln_2Fe_3O_7$.

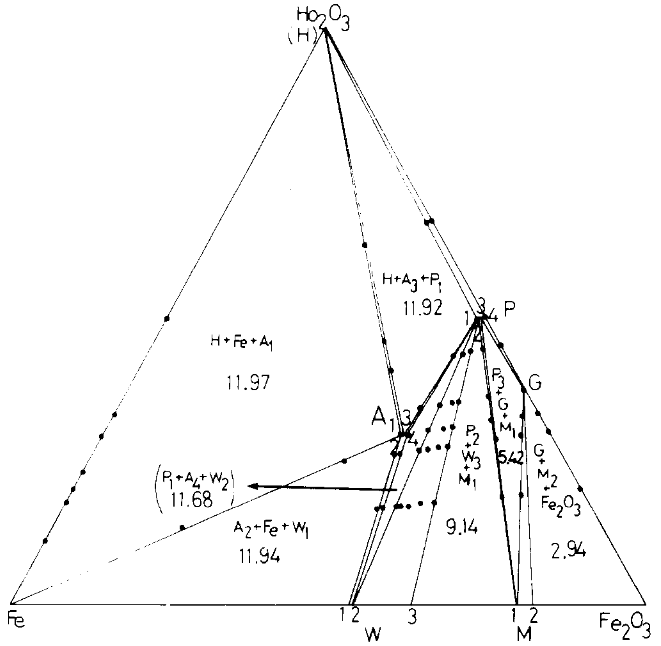

FIG. 2. The phase equilibria in the $Fe-Fe_2O_3-Ho_2O_3$ system at 1200°C. Numbers in the three solid fields mean the equilibrium oxygen partial pressure in terms of $-\log P_{O_2}$ (atm). Solid circles show the experimental results. Composition of each symbol is given in Table IIIa.

thermochemical properties of lanthanoid–iron–perovskite, $LnFeO_3$ (Ln = La, Nd, Sm, Eu, Gd, Tb, Dy, and Y) and pointed out that the standard Gibbs free energy of formation of $LnFeO_3$ at 1200°C from metallic iron, oxygen, and Ln_2O_3 is proportional to the tolerance factor defined by Goldschmidt *et al.* (*11*). Tretyakov *et al.* (*21–23*) reported independently the phase equilibria of Ce–Fe–O, Pr–Fe–O, and Eu–Fe–O systems at elevated temperatures.

The objectives of the present study are (i) to establish experimentally the phase equilibria in the $Fe–Fe_2O_3–Ho_2O_3$ and $Fe–Fe_2O_3–Tm_2O_3$ systems at 1150, 1200, and 1250°C, (ii) to determine the standard Gibbs free energies of formation of $Ln_3Fe_5O_{12}$ (Ln = Gd, Tb, and Dy) from metallic iron, oxygen, and Ln_2O_3 in order to complete the phase equilibria in the $Fe–Fe_2O_3$–(Gd, Tb, and Dy)$_2O_3$ systems, and (iii) to get the relationship between thermochemical and structural relative stabilities of $LnFeO_3$, $Ln_3Fe_5O_{12}$, $LnFe_2O_4$, and $Ln_2Fe_3O_7$.

Experimental

Guaranteed reagent grades of Fe_2O_3, Gd_2O_3, Tb_2O_3, Dy_2O_3, Ho_2O_3, Tm_2O_3, and Lu_2O_3 powders were employed for all starting materials. Each lanthanoid sesquioxide has the purity of more than 99.9%. Starting samples with desired ratios of Ln_2O_3/Fe_2O_3 were obtained by mixing them in an agate mortar under ethyl alcohol. Mixtures thus obtained were heated at 1200°C for 2–3 days in air.

Apparatus and procedures to control oxygen partial pressures, the criterion for determining the equilibrium state, the methods of both identification of the phases and chemical analysis of quenched samples, and the calculation method of the standard Gibbs free energy are just the same as those described in our previous papers (*1–7*).

Results and Discussion

(*1*) *Phase Equilibria*

(*a*) *The* $Fe–Fe_2O_3–Ho_2O_3$ *system.* Figure 2 illustrates the phase equilibria in the $Fe–Fe_2O_3–Ho_2O_3$ system at 1200°C. The following phases were stable under the present experimental conditions: Ho_2O_3, hematite (Fe_2O_3), magnetite (Fe_3O_4), wüstite (FeO), metallic iron (γ-Fe), holmium–iron–perovskite ($HoFeO_3$), holmium–iron–garnet ($Ho_3Fe_5O_{12}$), and $HoFe_2O_4$.

The Ho_2O_3 phase was stable under oxygen partial pressures ranging from 1 to 10^{-16} atm at 1200°C, and no significant nonstoichiometry was found in its composition. The $HoFeO_3$ phase had a detectable deviation from its stoichiometric composition. As seen in Fig. 2, the composition of the $HoFeO_3$ phase ranged from $HoFeO_{3.000}$ to $HoFeO_{2.955}$. However, the lattice constants of the $HoFeO_3$ phase with the same structure as those of $EuFeO_3$, $SmFeO_3$, $ErFeO_3$, and $LuFeO_3$ were almost identical irrespective of their variable

TABLE I

LATTICE CONSTANTS OF Ho–Fe–O COMPOUNDS SYNTHESIZED AT 1200°C

	Lattice constants			
Compound	*a* (Å)	*b* (Å)	*c* (Å)	*V* (Å^3)
$HoFeO_{3.00}$	5.280 ± 0.001 5.278[a]	5.587 ± 0.001 5.591[a]	7.604 ± 0.001 7.602[a]	224.3 ± 0.1 224.3[a]
$HoFe_2O_{3.878}$	3.519 ± 0.001		24.85 ± 0.01	266.4 ± 0.1
$HoFe_2O_{3.927}$	3.520 ± 0.001		24.83 ± 0.01	266.5 ± 0.1
$Ho_3Fe_5O_{12.00}$	12.378 ± 0.001 12.375[b]			1896.3 ± 0.1 1895.1[b]

[a] After Eibschutz (*19*).

[b] After Espinosa (*15*).

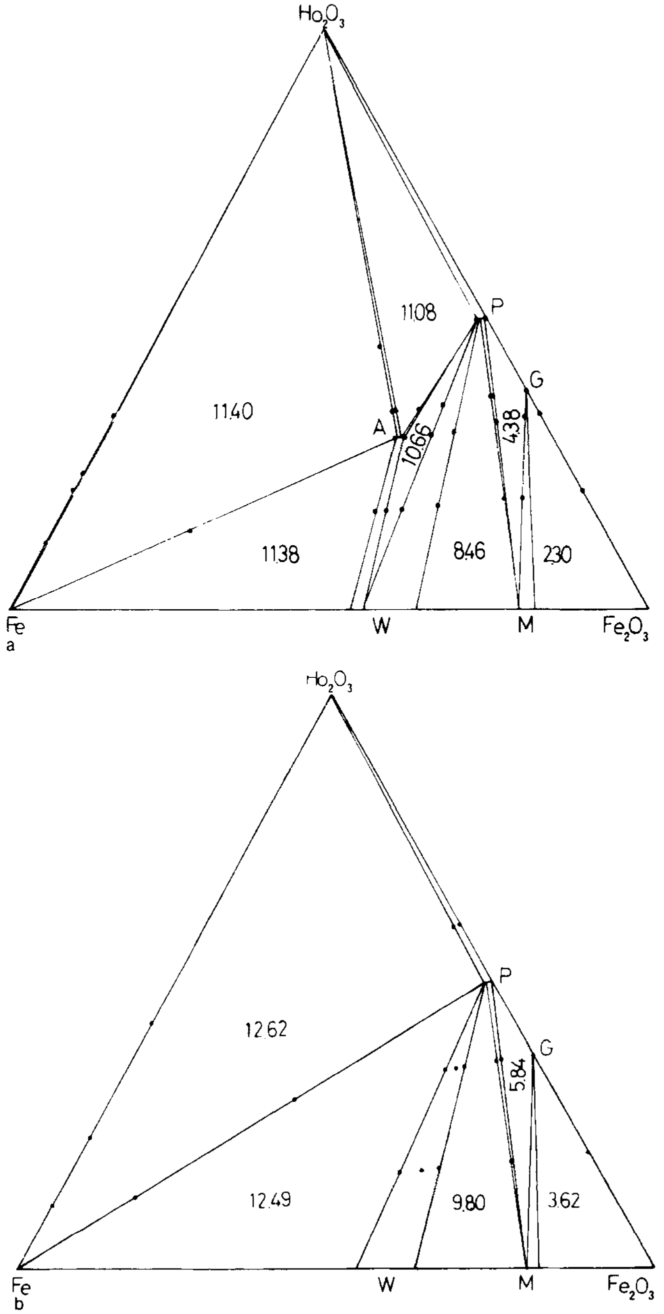

FIG. 3. (a) The phase equilibria in the Fe–Fe_2O_3–Ho_2O_3 system at 1250°C. (b) The phase equilibria in the Fe–Fe_2O_3–Ho_2O_3 system at 1150°C.

compositions. The $Ho_3Fe_5O_{12}$ phase had no significant deviation from the stoichiometric composition. The $HoFe_2O_4$ phase was stable in the narrowest range of oxygen partial pressures compared with any other phase of $LnFe_2O_4$ (Ln = Er, Tm, Yb, Lu, and Y). The compositional variation ranged from $HoFe_2O_{3.927}$ (A_1 in Fig. 2) to $HoFe_2O_{3.869}$ (A_4

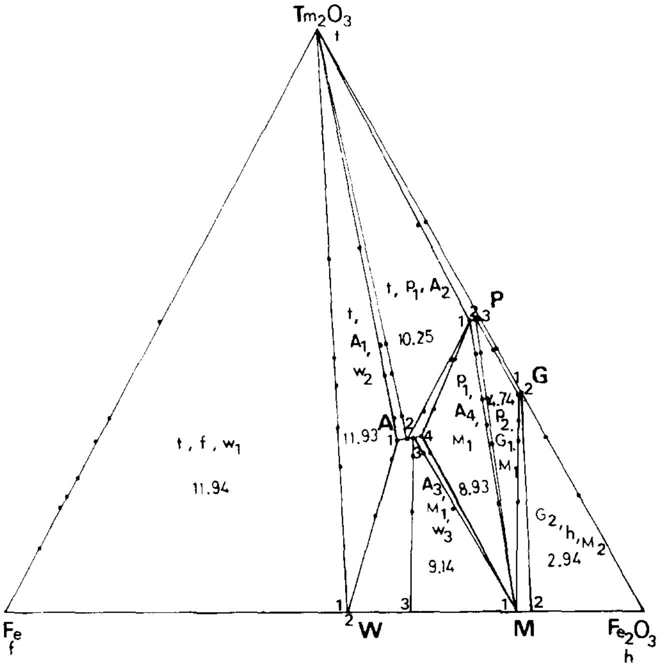

FIG. 4. The phase equilibria in the Fe–Fe_2O_3–Tm_2O_3 system at 1200°C. Composition of each symbol is given in Table IIIb.

in Fig. 2). The lattice constants of the $HoFe_2O_4$ phase are given in Table I as the hexagonal crystal system, together with those of $HoFeO_3$ and $Ho_3Fe_5O_{12}$. Figures 3a, b illustrate the phase equilibria in the same system at 1250 and 1150°C, respectively. As seen in Fig. 3a, the phase equilibria at 1250°C are the same as those at 1200°C with respect to the phase assemblage, except for values of the equilibrium oxygen partial pressures. The composition of the $HoFe_2O_4$ phase ranged from $HoFe_2O_{3.916}$ to $HoFe_2O_{3.867}$.

On the other hand, the phase equilibria in this system at 1150°C were essentially different from those at 1200 and 1250°C. This is seen in Fig. 3b. The $HoFe_2O_4$ phase disappeared at 1150°C, and therefore, the phase equilibria in the Fe–Fe_2O_3–Ho_2O_3 system at 1150°C should be transformed to the B type as seen in Fig. 1.

(*b*) *The Fe–Fe_2O_3–Tm_2O_3 system.* Figure 4 illustrates the phase equilibria in the Fe–Fe_2O_3–Tm_2O_3 system at 1200°C. The following phases were stable under the present experimental conditions: Tm_2O_3, hematite (Fe_2O_3), magnetite (Fe_3O_4), wüstite (FeO), metallic iron (γ-Fe), thulium–iron–perovskite ($TmFeO_3$), thulium–iron–garnet ($Tm_3Fe_5O_{12}$), and $TmFe_2O_4$.

Thulium sesquioxide (Tm_2O_3) was stable under oxygen partial pressures from 1 to 10^{-16} atm at 1200°C, and there was no significant nonstoichiometry in its composition. Thulium–iron–perovskite ($TmFeO_3$) had a range of nonstoichiometry as shown in Fig. 4. The lattice constants were, however, identical irrespective of its nonstoichiometry. The thulium–iron–garnet ($Tm_3Fe_5O_{12}$) also had a small but significant range of nonstoichiometry. The $TmFe_2O_4$ phase was stable under the low oxygen partial pressures ranging from $10^{-8.93}$ to $10^{-11.93}$ atm. The compositional variation of the $TmFe_2O_4$ phase was determined to be from $TmFe_2O_{4.022}$ to $TmFe_2O_{3.896}$. The lattice constants of the $TmFe_2O_4$ phase are given in Table II as the hexagonal crystal system, together with those of $TmFeO_3$ and $Tm_3Fe_5O_{12}$ phases. As seen in Table II, it is

TABLE II

LATTICE CONSTANTS OF Tm–Fe–O COMPOUNDS SYNTHESIZED AT 1200°C

Compound	Lattice constants			
	a (Å)	b (Å)	c (Å)	V (Å^3)
$TmFeO_{3.00}$	5.250 ± 0.001	5.571 ± 0.001	7.579 ± 0.001	221.6 ± 0.1
	5.251[a]	5.576[a]	7.584[a]	221.1[a]
$TmFe_2O_{3.911}$	3.480 ± 0.001		25.042 ± 0.004	262.6 ± 0.1
$TmFe_2O_{3.924}$	3.477 ± 0.001		25.037 ± 0.003	262.1 ± 0.1
$TmFe_2O_{3.970}$	3.474 ± 0.001		25.019 ± 0.002	261.5 ± 0.1
$TmFe_2O_{4.000}$	3.464 ± 0.001		25.057 ± 0.005	260.3 ± 0.1
$TmFe_2O_{4.010}$	3.462 ± 0.001		25.077 ± 0.005	260.3 ± 0.1
$Tm_2Fe_3O_7$[c]	3.499 ± 0.001		28.410 ± 0.004	301.2 ± 0.1
$Tm_3Fe_5O_{12.00}$	12.323 ± 0.001			1871.2 ± 0.1
	12.323[b]			1871.3[b]

[a] After Eibschutz (*19*).
[b] After Espinosa (*15*).
[c] Synthesized at 1380°C.

interesting to note that the c value in the lattice constants of the $TmFe_2O_4$ phase has a minimum value against its composition, and this was also the case in the $LuFe_2O_4$ phase (*6*).

The phase equilibria in the Fe–Fe_2O_3–Tm_2O_3 system at 1200°C are somewhat different from those of the other systems belonging to the C type in the sense of coexisting phase relations. First, thulium sesquioxide coexists with wüstite as shown in Fig. 4 and second, the $TmFe_2O_4$ phase coexists with magnetite under oxygen partial pressures ranging from $10^{-9.14}$ to $10^{-8.93}$ atm. These relations with respect to the coexisting phases are similar to the phase equilibria belonging to the D type, and thus the Fe–Fe_2O_3–Tm_2O_3 system at 1200°C seems to be of transitional phase equilibria between C and D types.

As seen in Fig. 5a, the phase equilibria in this system at 1250°C were the same in the picture as that at 1200°C. The composition of the $TmFe_2O_4$ phase ranged from $TmFe_2O_{3.879}$ to $TmFe_2O_{4.010}$ at 1250°C. Figure 5b illustrates the phase equilibria in this system at 1150°C. The $TmFe_2O_4$ phase had compositions between $TmFe_2O_{3.904}$ and $TmFe_2O_{4.003}$, and the Tm_2O_3 phase was not in equilibrium with wüstite at 1150°C.

It should be pointed out here that the phase equilibria in the Fe–Fe_2O_3–Ln_2O_3 (Ln = Ho, Er, and Tm) systems at 1200°C are gradually transformed to those of the D type in the sequence of the size of lanthanoid ions, and that the phase equilibria in the Fe–Fe_2O_3–Tm_2O_3 system change their picture to those of the D type when we increase the temperature as shown in Figs. 4, 5a, and 5b. This may suggest that an unknown compound $Tm_2Fe_3O_7$ may become stable at higher temperatures than 1250°C. Under this consideration, we tried to obtain the $Tm_2Fe_3O_7$ compound, and finally we have synthesized it at 1380°C and at an oxygen partial pressure of $10^{-7.48}$ atm (mixing ratio of CO_2/H_2 = 5.41). The lattice constants of the new compound $Tm_2Fe_3O_7$ are given in Table II, and every X-ray diffraction peak could be indexed according to the same crystal system of $Yb_2Fe_3O_7$ or $Lu_2Fe_3O_7$ (*9*).

(*c*) *Miscellaneous phase equilibria in the Fe–Fe_2O_3–Ln_3O_3 systems.* To complete the thermochemical studies of the Fe–Fe_2O_3–Ln_2O_3 (Ln = La, Nd, Sm, Eu, Gd, Tb, Dy, Ho, Er, Tm, Yb, Lu, and Y) systems, we determined the oxygen partial pressures at which

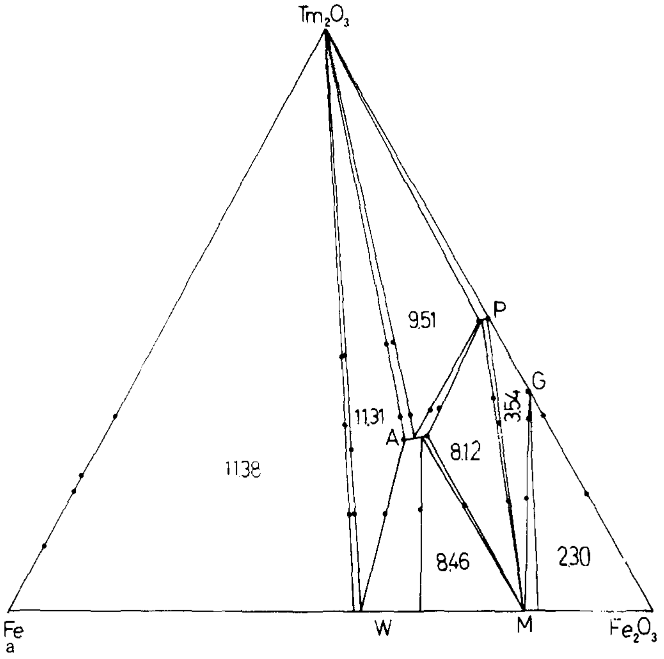

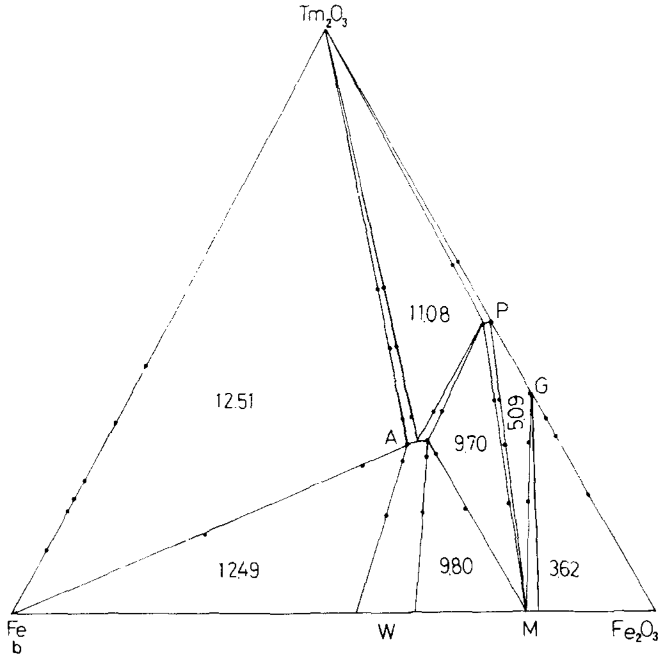

FIG. 5 (a) The phase equilibria in the Fe–Fe_2O_3–Tm_2O_3 system at 1250°C. (b) The phase equilibria in the Fe–Fe_2O_3–Tm_2O_3 system at 1150°C.

each garnet-type compound is in equilibrium with both perovskite and magnetite as written in the following equation:

$$\tfrac{2}{3}Fe_3O_4 + 3LnFeO_3 + \tfrac{1}{6}O_2 = Ln_3Fe_5O_{12}$$

where *Ln* includes only Gd, Tb, and Dy. These three are the members of the B type, and thus these data are sufficient to construct the phase equilibria because Katsura *et al.* (*2*) have determined the equilibrium oxygen partial pressures of the decomposition reactions related to the perovskite-type compounds. At 1200°C, the equilibrium oxygen partial pressures of the reaction for Gd, Tb, and Dy were determined to be $10^{-5.12}$, $10^{-5.83}$, and $10^{-5.53}$ atm, respectively. In these three garnet-type compounds, only the $Gd_3Fe_5O_{12}$ phase had a significant nonstoichiometry ranging from $Gd_3Fe_5O_{12.00}$ to $Gd_3Fe_5O_{11.97}$. In addition, we established the phase equilibria in the Fe–Fe_2O_3–Lu_2O_3 system at 1150 and 1250°C to compare these with the same system at 1200°C (*6*). The phase equilibria in this system at 1150 and 1250°C were the same in diagram as that at 1200°C.

(*d*) *Summary of phase relations for the* Fe–Fe_2O_3–Ln_2O_3 *systems at high temperatures.* It is correct that these systems at 1200°C are classified into four types based on the assembly of ternary compounds. However, as pointed out already in this paper, the classification depends greatly on temperature, and also, as found in the C and D types, each type of phase equilibria changes gradually its coexisting phase combinations. In connection with our studies, Tannieres (*12*) has studied the stability of $LnFe_2O_4$ and $LnFe_3O_7$ at 900 and 1000°C. According to her study, it may be concluded that the Fe–Fe_2O_3–Tm_2O_3 system at 1000°C, the Fe–Fe_2O_3–Yb_2O_3 system at 900°C, and the Fe–Fe_2O_3–Lu_2O_3 system at 900°C may belong to the C type, and the Fe–Fe_2O_3–Lu_2O_3 system at 1000°C may belong to the D type. Thus we can show conclusively the temperature dependence of each type at temperature intervals from 900 to 1400°C as illustrated in Fig. 6. From Fig. 6, it will be recognized that the B and C types change to C and D types at elevated temperatures, respectively, that is, Ho belonging to the B type changes to the C type at 1180°C, Tm which is a member of the C type at 1200°C changes to the D type at about 1350°C, and Lu belonging to the C type below 1000°C changes to the D type at higher temperatures. From this fact, it is suggestive to obtain an unknown compound $Ln_3Fe_4O_{10}$ [$(LnFeO_3)_3FeO$] and $Ln_4Fe_5O_{13}$ [$(LnFeO_3)_4FeO$]. Recently, Kimizuka *et al.* (*10*) have succeeded in synthesizing $Yb_3Fe_4O_{10}$ and $Yb_4Fe_5O_{13}$ at 1650°C and in CO_2 atmosphere.

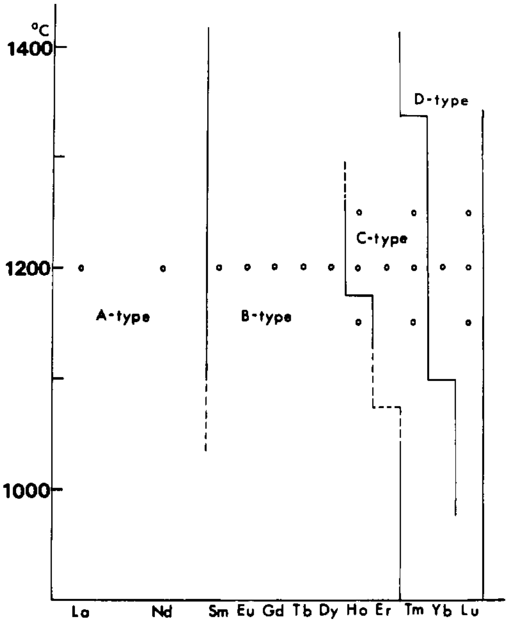

FIG. 6. Relationship between the phase assemblage and temperature in Fe–Fe_2O_3–Ln_2O_3 systems. The experimentally established phase diagrams are shown as open circles. Low-temperature area of Tm, Yb, and Lu was deduced from Tannieres (*12*).

(*2*) *Calculation of the Gibbs Free Energy of Formation of Ternary Compounds from Ln_2O_3, Metallic Iron, and Oxygen*

The method of calculations has been described in the previous papers (1–7), and here we will merely present the results of calculations in cases for Ho and Tm. The key

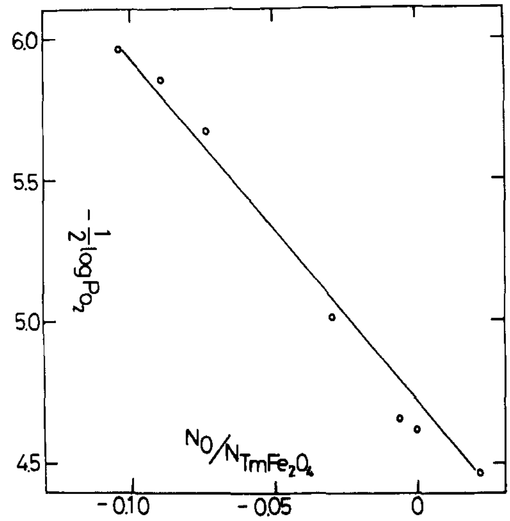

FIG. 7. Relationship between $-\frac{1}{2}\log P_{O_2}$ (atm) and $N_O/N_{TmFe_2O_4}$ at 1200°C.

points for calculations are as follows: Each compositional change of the $HoFe_2O_4$ and $TmFe_2O_4$ phases is small, and we could obtain the activity change being approximately linear with its composition. As an example, Fig. 7 shows the relationship between composition (in terms of $N_O/N_{TmFe_2O_4}$) and $-\frac{1}{2}\log P_{O_2}$ which makes it possible to calculate the $TmFe_2O_4$ activity at 1200°C. The calculated activity values are summarized in Tables IIIa and IIIb, and the standard Gibbs free energy values for Ho–Fe–O and Tm–Fe–O compounds at 1150, 1200, and 1250°C are given in Tables IVa and IVb, respectively.

(*3*) *Relative Stability of Compounds with the Same Crystal Structure*

Katsura *et al.* (*2*) have pointed out that the standard Gibbs free energy of formation of lanthanoid–iron–perovskite $LnFeO_3$ from Ln_2O_3, metallic iron, and oxygen changes proportionally with the tolerance factor defined by Goldschmidt *et al.* (*11*).

In this paper, we will apply the oxide–oxide reactions which do not involve the term of oxygen partial pressure.

(*a*) *Perovskite-type compounds.* We consider the standard Gibbs free energy change of the following reaction (1), ΔG^0 (1),

$$\tfrac{1}{2}Fe_2O_3 + \tfrac{1}{2}Ln_2O_3 = LnFeO_3. \qquad (1)$$

The standard Gibbs free energy of reaction (1) is easily calculated from the following reactions, (2) and (3):

$$Fe + \tfrac{1}{2}Ln_2O_3 + \tfrac{3}{4}O_2 = LnFeO_3, \qquad (2)$$

$$2Fe + \tfrac{3}{2}O_2 = Fe_2O_3. \qquad (3)$$

The standard Gibbs free energy of formation of Fe_2O_3 was cited from the JANAF Thermochemical Tables (*13*). ΔG^0 (1) values thus obtained are listed in Table Va. Figure 8 shows the relationship between $\Delta G^0(1)$ and the tolerance factor of $LnFeO_3$ defined by Goldschmidt *et al.* (*11*) [tolerance factor $t = (r_{Ln} + r_O)/2^{1/2}(r_{Fe} + r_O)$, where r_{Ln}, r_O, and r_{Fe} are ionic radii of Ln^{3+}, O^{2-}, and Fe^{3+}, respectively]. As seen in Fig. 8, the standard Gibbs free energy of reaction (1) is approximately proportional to the tolerance factor within the experimental errors, and the relationship is independent of temperature from 1150 to 1297°C.

(*b*) *Garnet-type compounds.* The following chemical reaction (4) was investigated and the standard Gibbs free energy change, $\Delta G^0(4)$, was obtained through reactions (5) and (6),

$$3LnFeO_3 + Fe_2O_3 = Ln_3Fe_5O_{12}, \qquad (4)$$

$$3LnFeO_3 + \tfrac{2}{3}Fe_3O_4 + \tfrac{1}{6}O_2 = Ln_3Fe_5O_{12}, \qquad (5)$$

$$\tfrac{2}{3}Fe_3O_4 + \tfrac{1}{6}O_2 = Fe_2O_3. \qquad (6)$$

The standard Gibbs free energy data of reaction (5), $\Delta G^0(5)$, have been determined by this and the previous studies (*1–7*), and that of reaction (6), $\Delta G^0(6)$, was cited from "JANAF" (*13*). The $\Delta G^0(4)$ values thus determined have somewhat larger experimental errors (± 0.6 kcal) than those of $LnFeO_3$.

As seen in Table Vb, the most stable lanthanoid–iron–garnet exists around the middle of the lanthanoid elements, and either lighter or heavier elements become more unstable thermochemically on the basis of the standard Gibbs free energy of reaction (4). Thus, it may be understandable that La– and

TABLE III

COMPOSITION–ACTIVITY RELATIONS

(a) Ho–Fe–O system

1150°C			1200°C			1250°C		
Composition	$-\log P_{O_2}$	$\log a_i$	Composition	$-\log P_{O_2}$	$\log a_i$	Composition	$-\log P_{O_2}$	$\log a_i$
$FeO_{1.048}$	12.49	0	$FeO_{1.048}$ $(W_1)^a$	11.94	0	$FeO_{1.050}$	11.38	0
$FeO_{1.159}$	9.80	−0.1394	$FeO_{1.070}$ (W_2)	11.68	−0.0069	$FeO_{1.077}$	10.66	−0.0192
			$HoFe_2O_{3.869}$ (A_1)	11.97	0	$HoFe_2O_{3.867}$	11.40	0
			$HoFe_2O_{3.879}$ (A_3)	11.92	0.0032	$HoFe_2O_{3.888}$	11.08	0.0196
			$HoFe_2O_{3.927}$ (A_4)	11.68	0.0148	$HoFe_2O_{3.916}$	10.66	0.0402
$HoFeO_{2.965}$	12.62	0	$HoFeO_{2.955}$ (P_1)	11.92	0	$HoFeO_{2.981}$	11.08	0
$HoFeO_{3.000}$		0	$HoFeO_{3.000}$ (P_4)		0	$HoFeO_{3.000}$		0
$Ho_3Fe_5O_{12.00}$	5.84	0	$Ho_3Fe_5O_{12}$ (G)	5.42	0	$Ho_3Fe_5O_{12.00}$	4.38	0

[a] Symbols in parentheses correspond to those in Fig. 2.

(b) Tm–Fe–O system

1150°C			1200°C			1250°C		
Composition	$-\log P_{O_2}$	$\log a_i$	Composition	$-\log P_{O_2}$	$\log a_i$	Composition	$-\log P_{O_2}$	$\log a_i$
$FeO_{1.048}$	12.49	0	$FeO_{1.048}$ $(W_1)^b$	11.94	0	$FeO_{1.050}$	11.38	0
$FeO_{1.159}$	9.80	−0.1394	$FeO_{1.052}$ (W_2)	11.93	0.0003	$FeO_{1.054}$	11.31	−0.0017
			$FeO_{1.165}$ (W_3)	9.14	−0.1435	$FeO_{1.172}$	8.46	−0.1566
$TmFe_2O_{3.904}$	12.51	0	$TmFe_2O_{3.896}$ (A_1)	11.93	0	$TmFe_2O_{3.879}$	11.31	0
$TmFe_2O_{3.954}$	11.08	0.0507	$TmFe_2O_{3.966}$ (A_2)	10.25	0.0579	$TmFe_2O_{3.953}$	9.51	0.0756
$TmFe_2O_{4.003}$	9.70	0.0654	$TmFe_2O_{4.022}$ (A_4)	8.93	0.0620	$TmFe_2O_{4.010}$	8.12	0.0885
$TmFeO_{2.980}$	11.08	0	$TmFeO_{2.977}$ (P_1)	10.25	0	$TmFeO_{2.977}$	9.51	0
$TmFeO_{3.000}$		0	$TmFeO_{3.000}$ (P_3)		0	$TmFeO_{3.000}$		0
$Tm_3Fe_5O_{12.00}$	5.09	0	$Tm_3Fe_5O_{11.98}$ (G_1)	4.74	0	$Tm_3Fe_5O_{12.00}$	3.54	0

[b] Symbols in parentheses correspond to those in Fig. 5.

TABLE IVa

THE STANDARD GIBBS FREE ENERGY VALUES FOR Ho–Fe–O COMPOUNDS

	Reactions	$-\Delta G^0$ (kcal)		
		1150°C	1200°C	1250°C
(1)	$Fe + \frac{1}{2}Ho_2O_3 + \frac{3}{4}O_2 = HoFeO_3$	61.6 ± 0.1	60.5 ± 0.2	59.2 ± 0.2
(2)	$Fe + \frac{1}{2}O_2 = FeO$	40.7 ± 0.1	40.2 ± 0.1	39.7 ± 0.1
(3)	$2Fe + \frac{1}{2}Ho_2O_3 + \frac{5}{4}O_2 = HoFe_2O_4$	—	100.9 ± 0.1	99.3 ± 0.1
(4)	$\frac{1}{2}HoFe_2O_4 + \frac{1}{4}Ho_2O_3 + \frac{1}{8}O_2 = HoFeO_3$	—	10.0 ± 0.1	9.6 ± 0.1
(5)	$FeO + HoFeO_3 = HoFe_2O_4$	—	0.15 ± 0.05	0.44 ± 0.05
(6)	$3FeO + \frac{1}{2}O_2 = Fe_3O_4$	34.6 ± 0.1	33.8 ± 0.1	32.75 ± 0.1
(7)	$3HoFeO_3 + \frac{2}{3}Fe_3O_4 + \frac{1}{6}O_2 = Ho_3Fe_5O_{12}$	6.3 ± 0.1	6.1 ± 0.1	5.6 ± 0.1
(8)	$5Fe + \frac{3}{2}Ho_2O_3 + \frac{15}{4}O_2 = Ho_3Fe_5O_{12}$	295.7 ± 0.7	290.5 ± 0.8	284.4 ± 0.8

TABLE IVb

THE STANDARD GIBBS FREE ENERGY VALUES FOR Tm–Fe–O COMPOUNDS

	Reactions	$-\Delta G^0$ (kcal)		
		1150°C	1200°C	1250°C
(1)	$2Fe + \frac{1}{2}Tm_2O_3 + \frac{5}{4}O_2 = TmFe_2O_4$	101.8 ± 0.1	100.6 ± 0.2	99.0 ± 0.2
(2)	$Fe + \frac{1}{2}O_2 = FeO$	40.7 ± 0.1	40.2 ± 0.1	39.7 ± 0.1
(3)	$2FeO + \frac{1}{2}Tm_2O_3 + \frac{1}{4}O_2 = TmFe_2O_4$	—	20.1 ± 0.1	19.7 ± 0.1
(4)	$\frac{1}{2}TmFe_2O_4 + \frac{1}{4}Tm_2O_3 + \frac{1}{8}O_2 = TmFeO_3$	8.85 ± 0.05	8.44 ± 0.05	8.02 ± 0.05
(5)	$TmFe_2O_4 + \frac{1}{6}O_2 = \frac{1}{3}Fe_3O_4 + TmFeO_3$	10.1 ± 0.1	9.6 ± 0.1	8.8 ± 0.1
(6)	$3FeO + \frac{1}{2}O_2 = Fe_3O_4$	34.6 ± 0.1	33.8 ± 0.1	32.75 ± 0.1
(7)	$3TmFeO_3 + \frac{2}{3}Fe_3O_4 + \frac{1}{6}O_2 = Tm_3Fe_5O_{12}$	5.5 ± 0.1	5.3 ± 0.1	4.1 ± 0.1
(8)	$Fe + \frac{1}{2}Tm_2O_3 + \frac{3}{4}O_2 = TmFeO_3$	59.7 ± 0.3	58.7 ± 0.3	57.4 ± 0.3
(9)	$5Fe + \frac{3}{2}Tm_2O_3 + \frac{15}{4}O_2 = Tm_3Fe_5O_{12}$	289.2 ± 0.8	284.5 ± 0.9	277.5 ± 0.9

Nd–iron–garnet are nonexisting compounds under the experimental conditions.

On the other hand, Euler and Bruce (*16*) have studied the structural analyses of garnet-type compounds and determined the relationship between the geometrical distortions of tetra-, octa-, and dodecahedra of oxygen ions and the coordinates of oxygen ion in the crystal. According to their conclusions, the degree of distortion of polyhedra is the result of the compromise between the minimum distortion and the shortened shared edges of the polyhedra. Then, the crystal-chemical stability of the garnet structure was explained in terms of both cone angle σ and azimuth ϕ, and these should be 54.74° and 0 in the most ideal structure, respectively. The values of σ and ϕ for the present lanthanoid–iron–garnet are cited in Table Vb. It may be seen from Table Vb that the values of σ for the lanthanoid–iron–garnet deviate from 54.74° with decreasing ionic radius from Sm to Lu, but, on the contrary, the values of ϕ approach zero with decreasing ionic radius. Thus, the contributions expected from both σ and ϕ are competitive. This may be in accord with the present thermochemical relative stability based on the standard Gibbs free energy of reaction (4).

(*c*) *LnFe$_2$O$_4$ and Ln$_2$Fe$_3$O$_7$ compounds.* We will consider reaction (7),

$$FeO + LnFeO_3 = LnFe_2O_4. \qquad (7)$$

Here, the standard free energy of formation of FeO is cited from the data by "JANAF" (*13*).

The results are given in Table Vc. The

TABLE Va

THE STANDARD GIBBS FREE ENERGY VALUES FOR EQS. (1) AND (2) RELATED TO $LnFeO_3$ (kcal/mole OF $LnFeO_3$)

	1150°C		1200°C		1224°C		1250°C		1297°C	
$LnFeO_3$	$-\Delta G^0$ (2)	$-\Delta G^0$ (1)	$-\Delta G^0$ (2)	$-\Delta G^0$ (1)	$-\Delta G^0$ (2)	$-\Delta G^0$ (1)	$-\Delta G^0$ (2)	$-\Delta G^0$ (1)	$-\Delta G^0$ (2)	$-\Delta G^0$ (1)
$LaFeO_3$			68.9 ± 0.1	15.7 ± 0.3			67.5 ± 0.1	15.7 ± 0.3	66.1 ± 0.1	15.6 ± 0.3
$NdFeO_3$			65.7 ± 0.1	12.5 ± 0.3			64.1 ± 0.1	12.4 ± 0.3	62.9 ± 0.1	12.4 ± 0.3
$SmFeO_3$			64.1 ± 0.1	10.9 ± 0.3			62.7 ± 0.1	10.9 ± 0.3	61.3 ± 0.1	10.8 ± 0.3
$EuFeO_3$			63.3 ± 0.1	10.1 ± 0.3	62.7 ± 0.1	10.2 ± 0.3	62.0 ± 0.1	10.2 ± 0.3	60.6 ± 0.1	10.1 ± 0.3
$GdFeO_3$			63.1 ± 0.1	9.9 ± 0.3	62.4 ± 0.1	9.9 ± 0.3	61.7 ± 0.1	9.9 ± 0.3	60.2 ± 0.1	9.7 ± 0.3
$TbFeO_3$	63.1 ± 0.1	8.4 ± 0.3	61.8 ± 0.1	8.6 ± 0.3	61.5 ± 0.1	9.0 ± 0.3	60.7 ± 0.1	8.9 ± 0.3		
$DyFeO_3$	62.4 ± 0.1	7.7 ± 0.3	61.2 ± 0.1	8.0 ± 0.3	60.8 ± 0.1	8.3 ± 0.3	59.9 ± 0.1	8.1 ± 0.3		
$HoFeO_3$	61.6 ± 0.1	6.9 ± 0.3	60.5 ± 0.2	7.2 ± 0.4			59.2 ± 0.2	7.4 ± 0.4		
$ErFeO_3$			59.8 ± 0.3	6.6 ± 0.4						
$TmFeO_3$	59.7 ± 0.3	5.1 ± 0.4	58.7 ± 0.3	5.5 ± 0.4			57.4 ± 0.3	5.6 ± 0.4		
$YbFeO_3$			58.2 ± 0.3	4.9 ± 0.5						
$LuFeO_3$	58.4 ± 0.3	3.7 ± 0.5	57.5 ± 0.3	4.3 ± 0.5			56.1 ± 0.3	4.3 ± 0.5		
$YFeO_3$			59.8 ± 0.2	6.0 ± 0.4						

TABLE Vb

THE STANDARD FREE ENERGY VALUES FOR EQS. (4) AND (5) RELATED TO $Ln_3Fe_5O_{12}$ (kcal/mole OF $Ln_3Fe_5O_{12}$), AND THE VALUES OF σ AND ϕ

	1150°C		1200°C		1250°C			
$Ln_3Fe_5O_{12}$	$-\Delta G^0$ (5)	$-\Delta G^0$ (4)	$-\Delta G^0$ (5)	$-\Delta G^0$ (4)	$-\Delta G^0$ (5)	$-\Delta G^0$ (4)	σ (°)	ϕ (°)
$Sm_3Fe_5O_{12}$			298.5 ± 0.8	1.3 ± 0.6			51.0 ± 0.2[a]	2.2 ± 0.2[a]
$Eu_3Fe_5O_{12}$			297.8 ± 0.8	2.0 ± 0.6				
$Gd_3Fe_5O_{12}$			298.2 ± 0.8	2.9 ± 0.6			50.6[b]	2.1[b]
$Tb_3Fe_5O_{12}$			294.9 ± 0.8	3.7 ± 0.6				
$Dy_3Fe_5O_{12}$			292.7 ± 0.8	3.4 ± 0.6			50.4[a]	1.8[a]
$Ho_3Fe_5O_{12}$	295.7 ± 0.7	3.0 ± 0.6	290.5 ± 0.8	3.3 ± 0.6	284.4 ± 0.8	2.8 ± 0.6		
$Er_3Fe_5O_{12}$			286.2 ± 0.8	2.3 ± 0.6				
$Tm_3Fe_5O_{12}$	289.2 ± 0.8	2.1 ± 0.6	284.5 ± 0.9	2.5 ± 0.6	277.5 ± 0.9	1.8 ± 0.6		
$Yb_3Fe_5O_{12}$			283.4 ± 0.9	3.3 ± 0.6			50.1 ± 0.1[a]	1.9 ± 0.2[a]
$Lu_3Fe_5O_{12}$			279.0 ± 0.9	1.4 ± 0.6			49.5 ± 0.2[a]	1.4 ± 0.3[a]
$Y_3Fe_5O_{12}$			288.9 ± 0.7	3.7 ± 0.6			50.3 ± 0.1[a]	1.8 ± 0.2[a]

[a] After Euler and Bruce (*16*).

[b] Calculated from the data by Weindemborner (*20*).

TABLE Vc

THE STANDARD GIBBS FREE ENERGY VALUES FOR EQS. (7) AND (8) RELATED TO $LnFe_2O_4$ AND $Ln_2Fe_3O_7$ (kcal/mole)

	1150°C		1200°C		1250°C	
$LnFe_2O_4$	$-\Delta G^0$ (7′)[a]	$-\Delta G^0$ (7)	$-\Delta G^0$ (7′)[a]	$-\Delta G^0$ (7)	$-\Delta G^0$ (7′)[a]	$-\Delta G^0$ (7)
$HoFe_2O_4$	—	—	100.9 ± 0.1	0.15 ± 0.05	99.3 ± 0.1	0.44 ± 0.05
$ErFe_2O_4$	—	—	100.8 ± 0.1	0.86 ± 0.05		
$TmFe_2O_4$	101.8 ± 0.1	1.4 ± 0.2	100.6 ± 0.2	1.7 ± 0.1	99.0 ± 0.2	1.0 ± 0.1
$YbFe_2O_4$			100.4 ± 0.2	2.0 ± 0.2		
$LuFe_2O_4$	101.4 ± 0.2	2.3 ± 0.2	100.3 ± 0.2	2.6 ± 0.2	98.6 ± 0.2	2.8 ± 0.2
YFe_2O_4			100.6 ± 0.1	0.54 ± 0.05		
$Ln_2Fe_3O_7$	$-\Delta G^0$ (8′)[b]	$-\Delta G^0$ (8)	$-\Delta G^0$ (8′)[b]	$-\Delta G^0$ (8)	$-\Delta G^0$ (8′)[b]	$-\Delta G^0$ (8)
$Yb_2Fe_3O_7$			158.4 ± 0.2	0.2 ± 0.2		
$Lu_2Fe_3O_7$	160.2 ± 0.2	0.3 ± 0.2	158.2 ± 0.2	0.3 ± 0.2	155.0 ± 0.2	0.3 ± 0.2

[a] Related to the equation, $2Fe + \frac{1}{2}Ln_2O_3 + \frac{3}{4}O_2 = LnFe_2O_4$ (7′).
[b] Related to the equation, $3Fe + Ln_2O_3 + 2O_2 = Ln_2Fe_3O_7$ (8′).

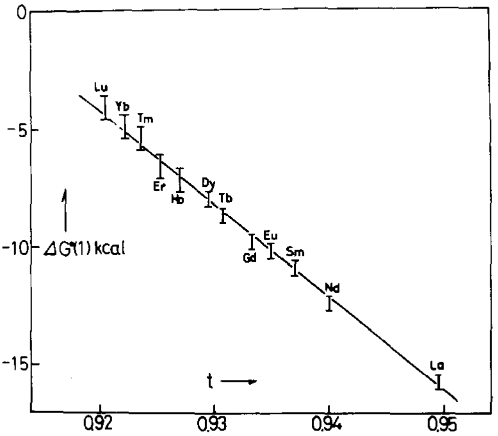

FIG. 8. Relationship between $\Delta G^0(1)$ and the tolerance factor t. The line attached to each lanthanoid element shows the range of the experimental errors.

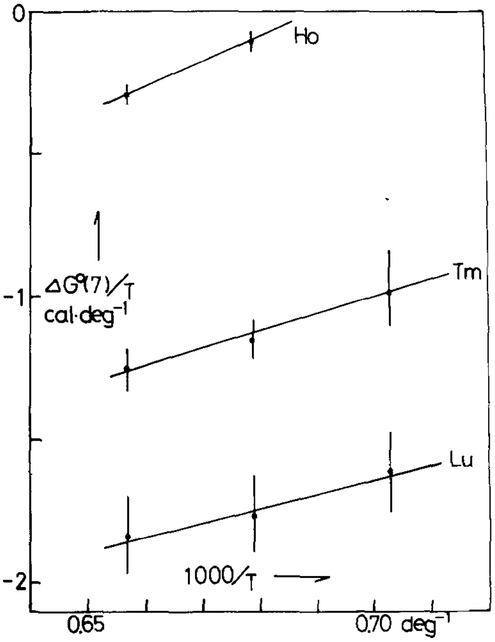

FIG. 9. Relationship between $\Delta G^0(7)/T$ and $1000/T$ in $LnFe_2O_4$ compounds. The lines mean the same as those in Fig. 8.

relationship between $\Delta G^0(7)$ and $1000/T$ is illustrated in Fig. 9, where T means the absolute temperature. The slope of each compound which means the standard enthalpy of reaction (7) is positive. Figure 10 shows the relationship between $\Delta G^0(7)$ and T. It is seen that the standard entropy change of reaction (7) is also positive. Thus, reaction (7) will occur more preferably at higher temperatures. This may be the case for Ho where $HoFe_2O_4$ was synthesized above 1200°C, but not at 1150°C. Figure 11 shows the relationship between $\Delta G^0(7)$ and the ionic radius of each lanthanoid ion from Shannon and Prewitt (*14*). As seen in Fig. 11, the $\Delta G^0(7)$ values at 1200 and at 1250°C are approximately proportio-

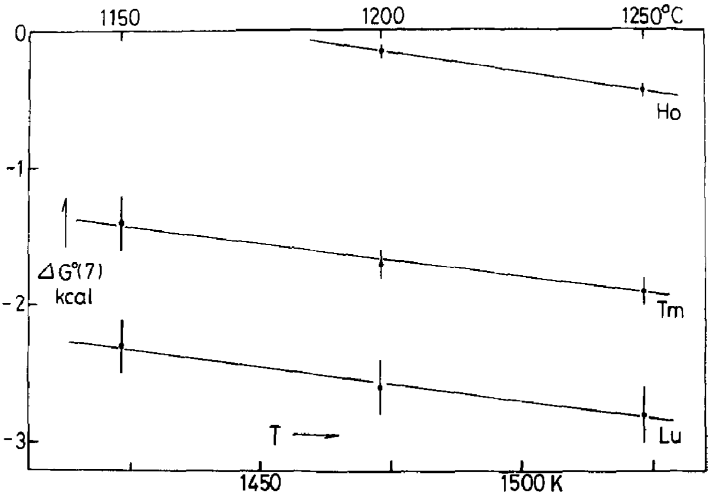

FIG. 10. Relationship between $\Delta G^0(7)$ and T in $Ln\mathrm{Fe_2O_4}$ compounds. The lines mean the same as those in Fig. 8.

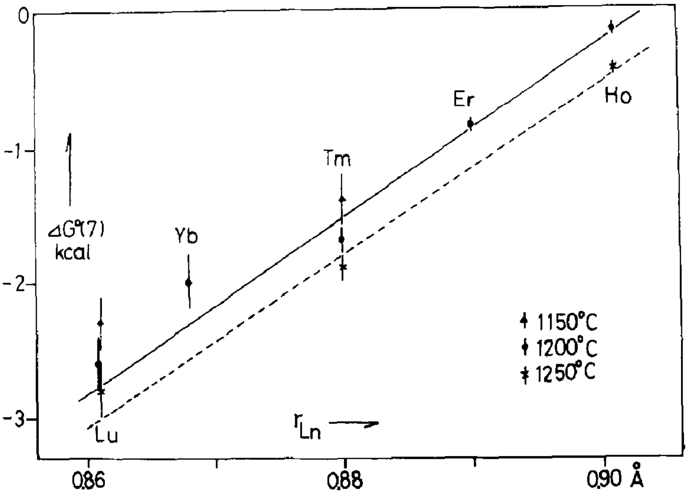

FIG. 11. Relationship between $\Delta G^0(7)$ and the ionic radii of lanthanoids in $Ln\mathrm{Fe_2O_4}$ compounds at 1200 (solid line) and 1250°C (broken line). Results at 1150°C are also plotted by solid triangles.

nal to the ionic radius. It is persuasive that the compound $\mathrm{DyFe_2O_4}$ will not be synthesized at 1200°C because of its positive standard Gibbs free energy of reaction (7).

For the series of $Ln_2\mathrm{Fe_3O_7}$ compounds, reaction (8) will be chosen to describe the thermochemical relative stability,

$$Ln\mathrm{Fe_2O_4} + Ln\mathrm{FeO_3} = Ln_2\mathrm{Fe_3O_7} \quad (8)$$

where Ln includes Yb and Lu. The standard Gibbs free energy change of reaction (8), $\Delta G^0(8)$, is easily calculated by using the data given in Tables IVa, b; Va, b, and c. The obtained results are given in Table Vc.

Magnetic and Mössbauer studies, and the neutron diffraction analyses for $(Ln\mathrm{FeO_3})_n\mathrm{FeO}$ ($n = 1, 2, 3,$ and 4) have partly been performed by Sugihara *et al.* (*17*) and by Bertaut (*18*), respectively, but the detailed properties of these compounds are still open to question.

Acknowledgment

The present authors thank the Ministry of Education, Japan, for a Grant-in-Aid (No. 14705, 1976).

References

1. N. KIMIZUKA AND T. KATSURA, *Bull. Chem. Soc. Japan* **47**, 1801 (1974).
2. T. KATSURA, K. KITAYAMA, T. SUGIHARA, AND N. KIMIZUKA, *Bull. Chem. Soc. Japan* **48**, 1809 (1975).
3. K. KITAYAMA AND T. KATSURA, *Bull. Chem. Soc. Japan* **49**, 998 (1976).
4. T. SUGIHARA, N. KIMIZUKA, AND T. KATSURA, *Bull. Chem. Soc. Japan* **48**, 1806 (1976).
5. N. KIMIZUKA AND T. KATSURA, *J. Solid State Chem.* **15**, 151 (1975).
6. T. SEKINE AND T. KATSURA, *J. Solid State Chem.* **17**, 49 (1976).
7. N. KIMIZUKA AND T. KATSURA, *J. Solid State Chem.* **13**, 176 (1975).
8. K. KATO, I. KAWADA, N. KIMIZUKA, AND T. KATSURA, *Z. Kristallogr.* **141**, 314 (1975).
9. K. KATO, I. KAWADA, N. KIMIZUKA, I. SHINDO, AND T. KATSURA, *Z. Kristallogr.* **143**, 278 (1976).
10. N. KIMIZUKA, K. KATO, I. SHINDO, I. KAWADA, AND T. KATSURA, *Acta Crystallogr.*, *B***32**, 1620 (1976).
11. V. M. GOLDSCHMIDT, T. BARTH, G. LUNDE, AND W. ZACHARIASEN, Pt. VII Skrifter Norske Videnskaps-Akad., Oslo, I. Mat. Naturv. KI, No. 2 (1926).
12. N. TANNIERES, Thèse présentee à l'université de Nancy I pour l'obtention du titre de docteur de spècialite (1974).
13. "JANAF Thermochemical Tables," 2nd ed., p. 37, NSRDS-NBS, 1971.
14. R. D. SHANNON AND C. T. PREWITT, *Acta Crystallogr. B***25**, 925 (1969). **26**, 1046 (1970).
15. G. P. ESPINOSA, *J. Chem. Phys.* **37**, 2344 (1962).
16. F. EULER AND J. BRUCE, *Acta Crystallogr.* **19**, 971 (1965).
17. T. SUGIHARA, M. ABE, AND T. KATSURA, *J. Phys. Soc. Japan* **40**, 1211 (1976).
18. E. F. BERTAUT, private communication.
19. M. EIBSCHUTZ, *Acta Crystallogr.* **19**, 337 (1965).
20. J. E. WEINDEMBORNER, *Acta Crystallogr.* **14**, 1051 (1961).
21. YU. D. TRETYAKOV, V. V. SOROKIN, A. R. KAUL, AND A. P. ERASTOVA, *J. Solid State Chem.* **18**, 253 (1976).
22. YU. D. TRETYAKOV, V. V. SOROKIN, AND A. P. ERASTOVA, *J. Solid State Chem.* **18**, 263 (1976).
23. YU. D. TRETYAKOV, V. V. SOROKIN, AND A. P. ERASTOVA, *J. Solid State Chem.* **18**, 271 (1976).
24. M. MAREZIO, J. P. REMEIKA, AND P. D. DERNIER, *Inorg. Chem.* **7**, 1337 (1968).